Available online at www.sciencedirect.com

ScienceDirect

Biochimica et Biophysica Acta 1768 (2007) 354–365

Biochimica et Biophysica Acta BBA

www.elsevier.com/locate/bbamem

Molecular studies of the gel to liquid-crystalline phase transition for fully hydrated DPPC and DPPE bilayers

Sukit Leekumjorn, Amadeu K. Sum *

Virginia Polytechnic Institute and State University, Department of Chemical Engineering, Blacksburg VA 24061, USA

Received 14 July 2006; received in revised form 1 November 2006; accepted 3 November 2006
Available online 11 November 2006

Abstract

Molecular dynamics simulations were used for a comprehensive study of the structural properties of saturated lipid bilayers, DPPC and DPPE, near the main phase transition. Though the chemical structure of DPPC and DPPE are largely similar (they only differ in the choline and ethanolamine groups), their transformation process from a gel to a liquid-crystalline state is contrasting. For DPPC, three distinct structures can be identified relative to the melting temperature (T_m): below T_m with "mixed" domains consisting of lipids that are tilted with partial overlap of the lipid tails between leaflet; near T_m with a slight increase in the average area per lipid, resulting in a rearrangement of the lipid tails and an increase in the bilayer thickness; and above T_m with unhindered lipid tails in random motion resulting in an increase in *%gauche* formed and increase in the level of interdigitation between lipid leaflets. For DPPE, the structures identified were below T_m with "ordered" domains consisting of slightly tilted lipid tails and non-overlapping lipid tails between leaflets, near T_m with minimal rearrangement of the lipids as the bilayer thickness reduces slightly with increasing temperature, and above T_m with unhindered lipid tails as that for DPPC. For DPPE, most of the lipid tails do not overlap as observed to DPPC, which is due to the tight packing of the DPPE molecules. The non-overlapping behavior of DPPE above T_m is confirmed from the density profile of the terminal carbon atoms in each leaflet, which shows a narrow distribution near the center of the bilayer core. This study also demonstrates that atomistic simulations are capable of capturing the phase transition behavior of lipid bilayers, providing a rich set of molecular and structural information at and near the transition state.

Keywords: Molecular dynamics; Phase transition; Gel; Liquid-crystalline; *Trans-gauche*; Isomerization; Interdigitation; DPPC; DPPE

1. Introduction

From recent studies, it has become apparent that both ordered and disordered lipid phases co-exist within eukaryotic cell membrane [1]. From a biological standpoint, several studies have suggested that ordered domains in cell membranes are closely associated with their function, including signal transduction [2,3], protein transport [2,4,5], and membrane sorting [2,4]. Other studies of these ordered domains have also suggested that they serve as a possible binding site for various pathogens and toxins [6–8]. Structurally, ordered domains are enriched with phospholipids, sphingolipids, and cholesterol. For example, several computational studies have shown a prominent role of cholesterol in membranes due to its introduced heterogeneity, creating ordered lipid domains and lipid rafts [9–11].

The ordered (gel) and disordered (liquid-crystalline) lipid phases have been a major focus in studies of the phase behavior of biological membranes, which relates the overall structural characteristics and dynamics of membranes to individual lipid components. Several experimental phase behavior investigations have been reported to characterize structural and dynamics properties of lipid bilayers in a gel, liquid-crystalline, and transition states. Suurkuusk et al. provided quantitative analysis based on calorimetric and fluorescent studies of uni- and multilamellar DPPC vesicles [12]. Their heating scan of multilamellar vesicles showed a transition process that closely resembled a first-order phase transition, which was confirmed by fluorescent measurements. For uni-lamellar vesicles, their heating scan showed significantly different phase behavior as two distinct endotherm peaks with subtle changes in the

* Corresponding author.
E-mail address: asum@vt.edu (A.K. Sum).

0005-2736/$ - see front matter © 2006 Elsevier B.V. All rights reserved.
doi:10.1016/j.bbamem.2006.11.003

fluorescence measurement during the phase transition were observed. Although these differences were identified between uni- and multi-lamellar vesicles, no clear explanation was provided to justify their findings. Davis used deuterium magnetic resonance to study the liquid-crystalline, gel phase, and phase transition of multi-lamellar labeled-DPPC vesicle [13]. His work provided quantitative measurements based on the deuterium spectra reported in term of the moments, which showed a sharp drop in the moment values upon heating the vesicle, a clear indication of a first-order transition. Huang and Li reported an extensive summary of studies of the main phase transition (gel to liquid-crystalline) of phospholipid bilayers using high-resolution differential scanning calorimetry (DSC) [14]. The lipids used in their investigation were saturated and unsaturated PC, PE, and PG (phosphatidylglycerol) with different acyl chain lengths. Based on their DSC measurements, a clear identification of a first-order phase transition was implied from the sharp endotherm peak in their heating scans of the bilayers. Nagle and Tristram–Nagle compiled studies of lipids at the liquid-crystalline state for DPPC, DMPC, DOPC, and DLPE containing structural data based on X-ray diffraction, NMR, and neutron scattering [15]. Their discussion also included a brief review of structural properties of DPPC at the gel, sub-gel, and ripple phases. Metso et al. provided an extensive DSC analysis and timed-resolved fluorescence spectroscopy to determine the nature of the phase transition of uni-lamellar DPPC liposomes [16], obtaining similar results to those by Suurkuusk et al. [12]. From their analysis, however, they attributed the subtle changes in fluorescence intensity at the phase transition for uni-lamellar bilayers to a second-order rather than a first-order phase transition. More recently, Kusube et al. investigated the phase transition of lipids at various temperatures and pressures [17] using DSC and light-transmittance to probe structural properties of DOPC, $DOMe_2PE$, DOMePE, and DOPE. With the results obtained they were able to produce various lipid phase diagrams along with enthalpy of formation and lipid molar volume at the transition point. They concluded that the difference in phase stability was mainly caused by the hydration and structure of the lipid headgroups.

A number of computational studies investigating the phase behavior of phospholipids have been reported using various modeling techniques, such as, Monte Carlo (MC) simulations [18–21], mean field theory [22], dissipative particle dynamics (DPD) simulations [23], atomistic [24–26] and coarse-grained (CG) [27,28] molecular dynamics simulations. Mouritsen et al. used MC simulations to study the first-order gel–fluid phase transition of lipids [18]. Since at that time there was only a limited number of thermodynamic properties at the transition state, they were the first to report the average lipid chain cross-sectional area, internal and free energies, coherence length, lateral compressibility, and specific heat. Nielson et al. also applied MC methods to investigate the phase behavior of single and multi-component membranes containing cholesterol [19]. However, their model was developed based on an off-lattice model with lipid and cholesterol molecules represented by hard-spheres. Their simulations provided consistent interpretation of a first-order phase behavior for pure lipid and lipid–cholesterol bilayer systems. Using a similar approach, Polson et al. studied the lateral diffusion of lipids across the main phase transition [20]. Their results suggested a significant change in the lateral diffusion of the lipids, which was found to be comparable to available experimental results. Later, Brannigan et al. investigated the phase behavior of a spherocylinder lipid model with MC simulations [21]. Their simulations showed distinct differences in the area per lipid and lateral diffusion coefficient between the solid and liquid phases. They also observed a third regime corresponding to a hexatic phase, a transition state between gel and liquid-crystalline phases, exhibiting intermediate values for the area per lipid and lateral diffusion coefficient. Chen et al. applied a macroscopic model based on the Gibbs potential to describe the transition state of lipids [22]. They reported the estimated values for phase transition temperature, enthalpy, van der Waals energy, number of *gauche* bonds, and chain orientational order parameter. The prediction using their model provided excellence agreement with experiment and thermodynamic properties such as internal energy and entropy of the system, which are inaccessible from experiments. Kranenburg et al. used DPD to study the phase behavior of lipid bilayers using model surfactants [23]. This technique allowed them to monitor the area per lipid and the bilayer thickness, both of which drastically changed at the phase transition from a gel to a liquid-crystalline phase.

Atomistic simulations of the phase transition for lipid bilayers are scarce. Heller et al. [24] and Venable et al. [25] performed MD simulations of lipid bilayers in both gel and liquid-crystalline states. Despite the short duration of the simulations, their results provided insight into several lipid properties, such as, internal pressure, lipid self-diffusion coefficient, order parameter, D-spacing (repeated spacing normal to bilayer), chain tilt, and *%gauche*. Recently, de Vries et al. performed a detailed MD study of the phase behavior of lecithin (DPPC) using atomistic models [26]. Their simulation showed a spontaneous formation of a ripple gel phase upon cooling of a fully hydrate DPPC bilayer below the main phase transition temperature. More recently, there have been a number of studies based on CGMD models to investigate the phase behavior of lipids. Stevens showed that DPPC bilayers have tilted lipid chains at low temperatures [27]. Moreover, the simulations indicated a large hysteresis in the area per lipid and bilayer thickness in heating and cooling cycles of the lipid bilayer, resulting in conditions difficult to identify the phase transition. In another CG study, Marrink et al. investigated a gel phase formation for DPPC membranes [28]. They suggested a four-stage reversible process from a gel to a liquid-crystalline phase: nucleation, growth, limited growth, and optimization. Their simulations yielded a main phase transition at about 295 ± 5 K and a lateral diffusion coefficient in the order of 1×10^{-9} cm^2/s.

Coarse-grained models are better suited to obtain insight into the properties of order domains in relation to lipid rafts, as large bilayers and long simulation times can be achieved to model large-scale properties of membranes. This was the approach by Marrink et al., in which a CG model clearly showed the transformation process associated with a phase transition [28].

However, CG models are unable to capture molecular features and characteristics of the lipid molecules and more subtle structural properties of bilayers. As such, atomistic simulations for the transition state may establish additional information to understand the properties of lipid domains. Here, we present a series of MD simulations for DPPC and DPPE bilayers to determine the possible mechanisms underlying the phase transition process.

2. Simulation details

Two sets of lipid bilayers were considered here: one with 128 lipids (64 per leaflet) and another with 256 lipids (128 per leaflet). Although the size of the bilayers remains relative small compared to previous simulations with coarse-grained models, they are significantly larger than those used in other atomistic simulations studying phase transitions. Moreover, as it will be shown in the discussion, the results seem insensitive to doubling the bilayer size to 256 from 128 lipids. We also performed two sets of simulations to investigate the changes occurring to the bilayers as a function of temperature. To mimic experimental phase transition studies, the first set of simulations initially equilibrated the bilayer systems through a series of annealing steps from 250 to 350 K (heating), followed by the reverse path from 350 to 250 K (cooling), thus tracing the hysteresis curve of melting. These temperature ranges were chosen to include the main phase transition from a gel to a liquid-crystalline phase of both DPPC and DPPE, which have experimental values of ~315 K and 337 K, respectively [29,30]. For these simulations, the initial structures were obtained from previously equilibrated bilayers at 250 K and 350 K for the heating and cooling simulations, respectively. The heating and cooling rates used were 2.5 K per ns. As it will be shown, the selected rate is adequate to obtain a number of structural properties that allow us to identify the transitional process from a liquid ordered to a liquid disordered state, and vice-versa. The annealing runs were performed with both small and large lipid bilayer systems.

In addition to the annealing runs, we performed separate simulations of the lipid bilayers at fixed temperatures above and below the phase transition, amounting to a total of 16 configurations, as summarized in Table 1. Each configuration was processed through a series of heating and cooling steps from the desired temperatures to 450 K and back to erase any hysteresis of the systems prior to the start of each simulation. Beyond the equilibration, a total simulation time of 50 ns were collected for each system, of which the last 20 ns were used in the evaluation of the equilibrium properties.

Because periodic boundary are imposed on the systems in the simulations, the bilayer configuration is essentially that of a multi-lamellar system. It is known that uni and multi-lamellar bilayers exhibit different phase behavior [12]. To minimize the periodicity of a multi-lamellar systems, the systems considered contained 40 water/lipid, which is above the swelling limit proposed by Nagle and Tristran–Nagle [15], thus making the systems to behave closer to uni-lamellar configurations.

Table 1
Composition and temperature for the bilayer systems considered in the fixed temperature simulations

System	Lipid/leaflet	Water	Temperature (K)
DPPC	64	5,120	250, 280, 290, 300, 310, 320, 330, 340, 350
DPPE	64	5,120	290, 300, 310, 320, 330, 340, 350

A total of 128 lipids were used for all systems.

The force field for DPPC, DPPE, and water are consistent with those employed in a previous study [31], which includes intramolecular parameters for bonds, angles, proper dihedral, and improper dihedral [32,33]. The Ryckaert–Bellemans potential was used for the torsion potential of the lipid hydrocarbon chains [34]. Non-bonded interactions were described by the parameters from Berger et al. [35–37] and partial atomic charges were obtained from Chiu et al. [38]. The single point charge (SPC) model was adopted for water [39]. The united-atom representation was used for the methyl/methylene groups in the acyl chains of both DPPC and DPPE.

All simulations were performed in the *NPT* ensemble, at a pressure of 1 bar and at various temperatures between 250 and 350 K. (see ref. [31] for more details on the parameters used in the simulations). A time-step of 2 fs was used for all simulations. Coulombic and van der Waals interactions were cutoff at 9 Å. Long-range electrostatic interactions were corrected with the particle-mesh Ewald method (PME) [40,41] (0.10 nm for the grid size, fourth-order spline interpolation, and real-space cutoff at 9 Å). Trajectories were collected every 2 ps. All simulations were performed with the GROMACS 3.3 software package [42,43] (single-precision mode) in parallel using Virginia Tech's System X (dual 2.3 GHz Apple Xserve G5) [44].

3. Results and discussion

The main focus of this study is to obtain a better understanding of the phase transition of DPPC and DPPE bilayers. Note that the lipid force field employed here was developed for the liquid-crystalline phase, and as such, it was unclear at first whether it was suitable to represent gel phase properties. In the first set of simulations, we considered the small bilayer system (128 lipids) to validate the properties of the bilayers near their transition state. To accomplish this task, we performed a series of heating and cooling scans of each lipid bilayer system starting from previously equilibrated structures at 250 K and 350 K, respectively. Several annealing simulations were conducted with different starting configurations and initial velocities to improve the statistical analysis of the results. The structural properties considered for this analysis were the area per lipid and the bilayer thickness, both of which are sensitive to the phase state of the bilayer [45]. The average area per lipid was calculated from the cross-sectional area of the simulation box (plane along the bilayer surface, *xy*-plane) divided by the number of lipids per leaflet (64 lipids). The bilayer thickness is quantified from the distance of the mean position of the phosphorus atoms in each leaflet. Figs. 1 and 2 shows the approximate area per lipid and bilayer thickness, respectively, resulting from the heating and cooling scans of the DPPC and DPPE bilayers. From Fig. 1, the heating scans of both DPPC

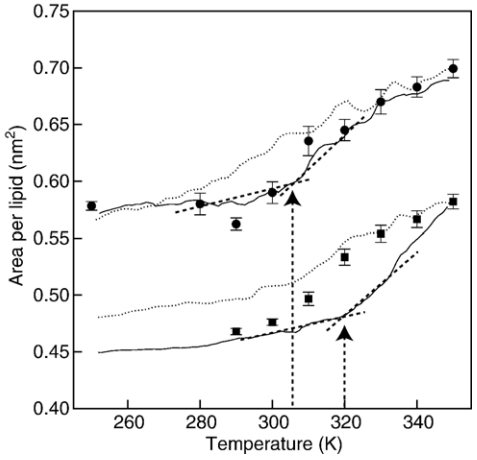

Fig. 1. Area per lipid obtained from annealing and fixed temperature simulations. Solid and dotted lines correspond to the heating and cooling scans, respectively, for DPPC (top data) and DPPE (bottom data). Heating and cooling rates of 2.5 K/ns were used to obtain the hysteresis loop. Circles and squares are results for DPPC and DPPE, respectively, from the fixed temperature simulations. Error bars are estimated standard deviation.

and DPPE show a transition point around 305 K and 320 K, respectively, which corresponds to the temperature in which there is a change in the slope of the heating curves. However, for the cooling scans, the identification of a phase transition is not as clear, as the area per lipid decreases more gradually with decreasing temperature. Similar results are observed in Fig. 2 for the bilayer thickness: the phase transition can be easily identified in the heating scans, but less clearly in the cooling scans. The heating and cooling scans shown in Figs. 1 and 2 represent hysteresis loops, a prominent characteristic of any system undergoing a first-order phase transition. This type of behavior for lipid bilayer is actually seen from several experimental [12–14] and computational [19,23,27] studies which supports a first-order phase transition mechanism. One of the reason the heating and cooling do not form a closed-loop is because we used the same annealing rate for heating and cooling, and the process from a disordered to ordered state is much more susceptible to metastability than the reverse path. Although the phase transition temperatures obtained for both DPPC and DPPE are below the experimental values, the results presented thus far are an affirmation of the phase behavior of lipid bilayers and the molecular changes associated with phase transformations. In a second set of simulations, we considered a larger bilayer (256 lipids) to determine whether the results were dependent on the system size, since phase transition is a cooperative phenomena. To verify this, annealing simulations were performed with the same settings for the small bilayer, that is, heating and cooling scans with a rate of 2.5 K/ns (see Fig. S1 in the Supplementary material). The results of these additional simulations demonstrated consistent results between the small and large bilayers, thus assuring that the observations with the small bilayer yielded acceptable properties for phase transformations. Based on these results, we proceeded to look more closely the equilibrium properties of the lipid bilayer systems at various temperatures near the phase transition.

Figs. 3 and 4 show a series of snapshots from the MD trajectories of DPPC and DPPE bilayers, respectively, at various temperatures (see Table 1 for more information). For clarity, two separate views are shown, one corresponding to the *xz*-plane and another to the *yz*-plane of the simulation box (*z*-axis is along the bilayer normal). For DPPC, two distinct domains are observed between 250 and 300 K, as shown in Fig. 3. The first domain consists of lipids that are fully stretch with no overlap between lipid tails from the adjacent leaflet, which will be referred as the "ordered" domain. The second domain is identified as the overlapping section of lipid tails from each leaflet, and will be referred as the "disordered" domain. We see from the snapshots that the lipid tails are tilted in the "ordered" domain and partially overlap in the "disordered" domain. This type of lipid alignment has been previously reported as a ripple phase in lecithin by de Vries et al. [26]. Since the bilayer systems presented here are too small to form a ripple phase, we will refer them as a "mixed" domain. To verify the stability of these structures, we instantaneously heated and cooled the system in an annealing process to ensure that the resulting structures were not in a metastable state. This was accomplished by heating the system to 450 K and then cooling it to the respective temperature in the *NVT* ensemble. At the desired temperature, systems were equilibrated for at least 10 ns before production runs. At the higher temperatures (T = 310 K), the lipid tails of DPPC are fully random, which is characteristic of a liquid-crystalline phase. A similar procedure was applied to DPPE. For DPPE, only the "ordered" domain with tilted lipid chains was observed between 290 and 310 K, as shown in Fig. 4. In these cases, all lipid tails are tightly packed, with less interdigitation between them. Compared to DPPC, the "mixed" phase behavior in DPPE is not observed from the simulations because the "ordered/disordered" patterns

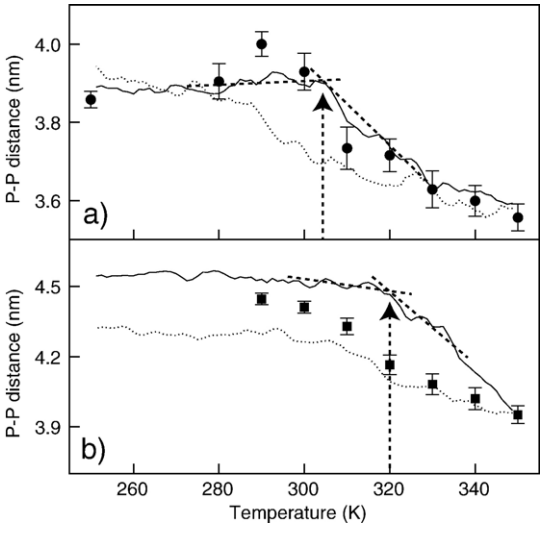

Fig. 2. Bilayer thickness obtained from annealing and fixed temperature simulations. Solid and dotted lines correspond to the heating and cooling scans, respectively, for (a) DPPC and (b) DPPE. Heating and cooling rates of 2.5 K/ns were used to obtain the hysteresis loop. Circles and squares are results for DPPC and DPPE, respectively, from the fixed temperature simulations. Error bars are estimated standard deviation.

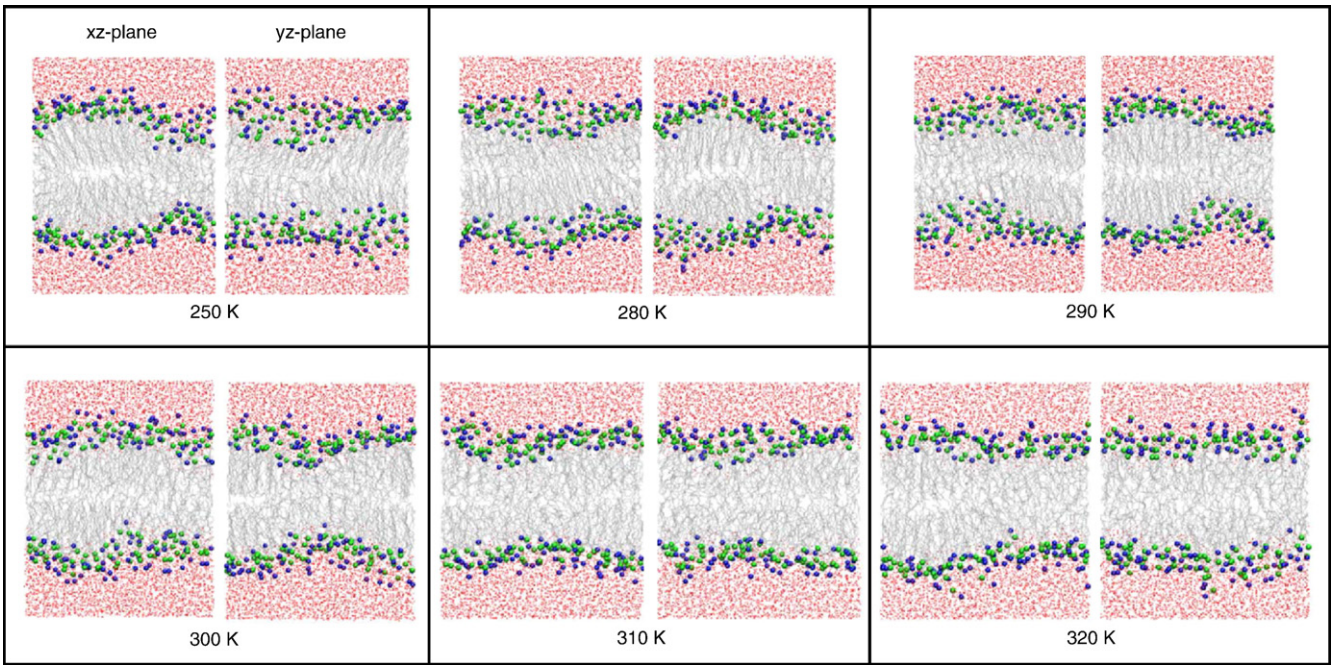

Fig. 3. Snapshots of DPPC bilayers at various temperatures. Views of the simulation boxes are shown for both *xz*- and *yz*-planes. *z*-axis is normal to the bilayer interface. The bilayer core region is centered in the middle of the snapshots.

seem absent. This is consistent with the experimental study by Yao et al. [46], in which they were unable to distinguish a stable phase from a gel to a liquid-crystalline phase for DPPE using X-ray scattering, unlike the case for DPPC. Even though the experiments by Yao et al. were insufficient to provide insight into the phase transition mechanism of DPPE, our results suggest that DPPE undergoes a phase transition without existing as a "mixed" domain. Further quantitative measurements are given in the following sections to determine the structural changes associated with each phase.

A number of properties were analyzed to characterize and quantify the changes in the bilayer structure with respect to the phase transition temperature for DPPC and DPPE, including: area per lipid, bilayer thickness, lipid tail tilt-angle, lipid tail order parameter, hydrocarbon *trans-gauche* isomerization, and level of interdigitation. These properties were obtained from the ensemble average of the trajectories over the last 30 ns of the simulations for each system listed in Table 1. The stability of each system was monitored by the average area per lipid (see Fig. S2 in the Supplementary Material).

For the lipid bilayer systems at the lower temperatures, we observed that the bilayer surface showed abnormal defects resulting from the rigidity and packing of the phospholipids. As such, it was unclear that the area per lipid for those systems can be quantified appropriately. Note that these defects were absent at higher temperatures (see Figs. 3 and 4). As shown in Fig. 1, the area per lipid of the bilayers at the different temperatures showed consistent agreement with the annealing simulations, with the exception of the data at 290 K for DPPC that deviated from the expected value. The average area per lipid for DPPC increases almost linearly with temperature above 310 K. A similar linear relationship was reported by Sum et al. for DPPC in the liquid-crystalline state [47]. At the lower temperatures, the average area per lipid for DPPC is more scattered due to the "mixed" domains exhibited by the many stable configurations of the systems. That is, the average area per lipid significantly increases when the lipid tails are predominantly tilted with large tilt-angle and decreases when they are tightly packed with the lipid tails aligned parallel to the bilayer normal. Our finding agrees well with previous X-ray diffraction experiments on fully hydrated DPPC by Ruocco et al. that observed a tilted lipid arrangement in the gel phase and a more parallel alignment to the bilayer normal near the transition point [48]. For DPPE, because the "mixed" domains seem absent from the structures (see Fig. 4), the average area per lipid obtained from the individual simulations is between the values obtained from annealing simulations. Further analysis, as presented below, is needed to obtain a better understanding of the bilayer structures near the phase transition.

As shown in Fig. 2, the bilayer thickness was also compared between the annealing simulations and simulations of the bilayers at different temperatures. The bilayer thickness was calculated from the distance between the average position of the phosphorus atoms in each leaflet. The results for both DPPC and DPPE yield similar trends with a decrease in the bilayer thickness accompanying the phase transition from an ordered to a disordered state. This also verifies that the system size and the heating rate chosen are sufficient to describe the phase behavior near the main transition state. A closer inspection of the results for DPPC in Fig. 2a indicates a slight increase in bilayer thickness prior (at 290 K) to the phase transition temperature. This increase in the bilayer thickness is related to the change in the alignment of the lipid tails from a "mixed" to an "ordered" phase, causing the bilayer to expand. A similar behavior is not observed for DPPE (see Fig. 2b) because a "mixed" phase seem absent. Additional analysis to

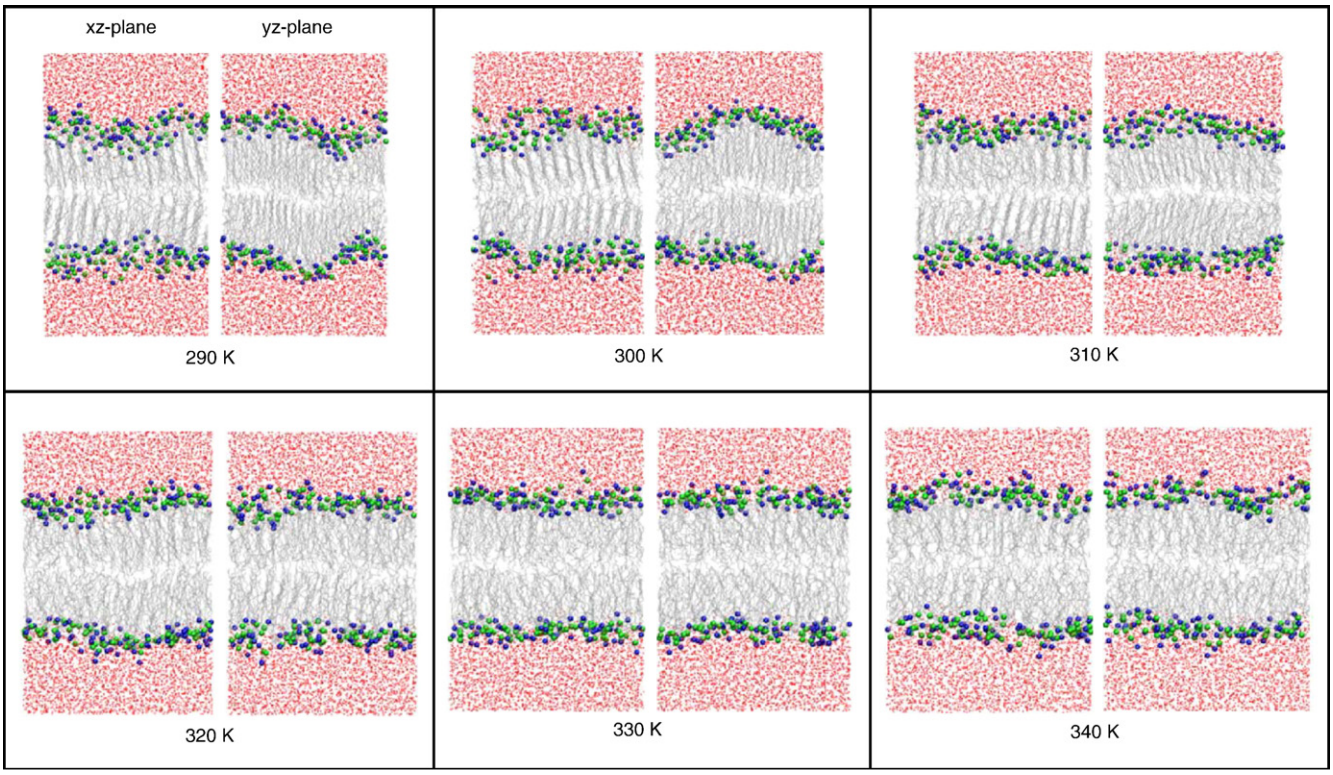

Fig. 4. Snapshots of DPPE bilayers at various temperatures. Views of the simulation boxes are shown for both *xz*- and *yz*-planes. *z*-axis is normal to the bilayer interface. The bilayer core region is centered in the middle of the snapshots.

verify the alignment of the lipid tails is given in the next section.

In Fig. 3, we observed configurations with "mixed" domains below the melting temperature (T_m), which in turn resulted in a bilayer with uneven thickness. As discussed in the previous paragraph, the DPPC structure experienced a noticeable increase in the bilayer thickness below T_m , which corresponded to a transformation from a cross-tilted (Fig. 5a) to a tilted lipid arrangement (Fig. 5b). This rearrangement causes a slight increase in the area per lipid near T_m (see Fig. 2a), as the lipid molecules align perpendicular to the bilayer surface at temperatures near the phase transition, which in turn causes a slight increase in the bilayer thickness upon heating the bilayer. Once T_m has reached, the lipid tails become interdigitated, resulting in a decrease of the bilayer thickness and an increase in the area per lipid (see Fig. 5c).

Although this cooperative phenomena is observed, the analysis suggests that an increase in the area per lipid is an essential step to induce a rearrangement of lipid molecules before transforming to a liquid-crystalline phase. Unlike DPPC, DPPE bilayers are predominantly in the "ordered" phase with little tilt of the lipid tails below T_m . Therefore, the rearrangement of DPPE is minimal and the bilayer thickness slightly reduces until it reaches the phase transition temperature.

To further verify the structural transformation of DPPC and DPPE during the phase transition, we analyzed the lipid tail tilt-angle with respect to the bilayer normal. Note that for this analysis, we used the single temperature simulations listed in Table 1. One measure of a lipid bilayer in a liquid-crystalline state is that the lipid tails are fully random and unhindered to take any orientation within the bilayer. If the bilayer exhibits a preferred orientation (ordered domains), as the low temperature structures shown in Figs. 3 and 4, it is considered to be in a gel state. We calculated the angle distribution of each carbon segment in the lipid tails with respect to the bilayer normal to determine the orientation of the lipids in the bilayer. The carbon segment, in this case, refers to a vector between alternate carbon units along the lipid tail, as shown in Fig. 6. Note that the angle can be either positive or negative depending on the alignment of lipid tails (a zero degree corresponds to a vector pointing along the bilayer normal direction). As seen in Figs. 3 and 4, the alignment of the lipid tails are significantly different whether

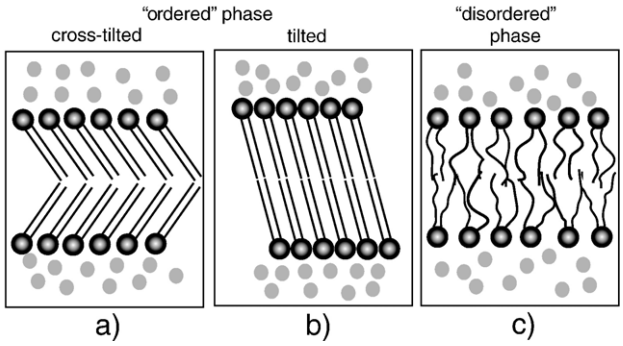

Fig. 5. Schematic representation of the lipid alignment in the "ordered" and "disordered" phases: (a) cross-tilted, (b) tilted, and (c) random. Both tilted and cross-tilted alignments are observed in the gel phase (see Figs. 3 and 4). Black and gray spheres represent the lipid headgroup and water, respectively.

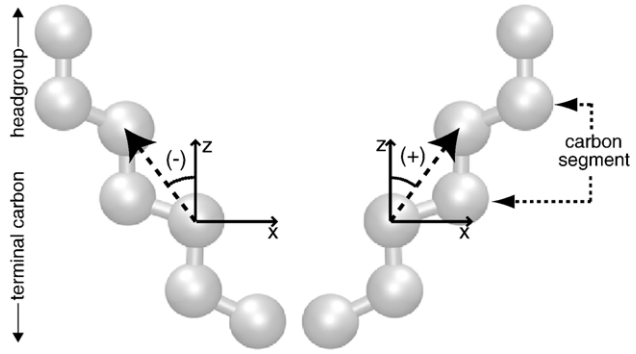

Fig. 6. Pictorial representation of the vector formed by alternating carbon units along the lipid tails. The positive (+) and negative (−) tilt-angles are measured with respected to the *z*-axis (zero degree). Note that only the *xz*-plane is shown in the figure for clarity. A similar tilt-angle can be defined in the *yz*-plane.

viewed from the *xz*- or *yz*-plane, and as such, the angle distributions are calculated for both planes. Fig. 7 shows the normalized tilt-angle distribution for DPPC and DPPE. There are three distinct structural alignments of the lipids that can be used to determine the phase transition point. In the gel phase, we observe two of these structures: one produces the double peak in the distribution and the other shows a narrow angle distribution. In the liquid-crystalline phase, we observe a wide distribution centered around zero degree. Our analysis indicates that the double peak refers to the cross-tilted lipid arrangement shown in Fig. 5a. The narrow distribution implies that the lipid tails are predominantly tilted to some degree, as illustrated in Fig. 5b. A wide distribution centered at around zero degree indicates that the lipid tails are fully random (Fig. 5c). To quantify the phase change from the distribution curves, we calculated the full-width of the distribution at half-height of the peak maximum (FWHH). The systems with the double peaks were not considered in this calculation as they introduce biased results; these include DPPC at 250 K (Fig. 7a and b) and DPPE at 290 K (Fig. 7c). Fig. 8 shows the calculated FWHH of the distributions with respect to the temperature. For DPPC, there is a significant jump in the FWHH value from 300 to 310 K (see Fig. 8a). This shows that the tilted alignment of the lipids significantly reduces in this temperature range. Again, this is consistent with our previous analysis and we conclude that the phase transition temperature for DPPC occurs between 300 and 310 K. For

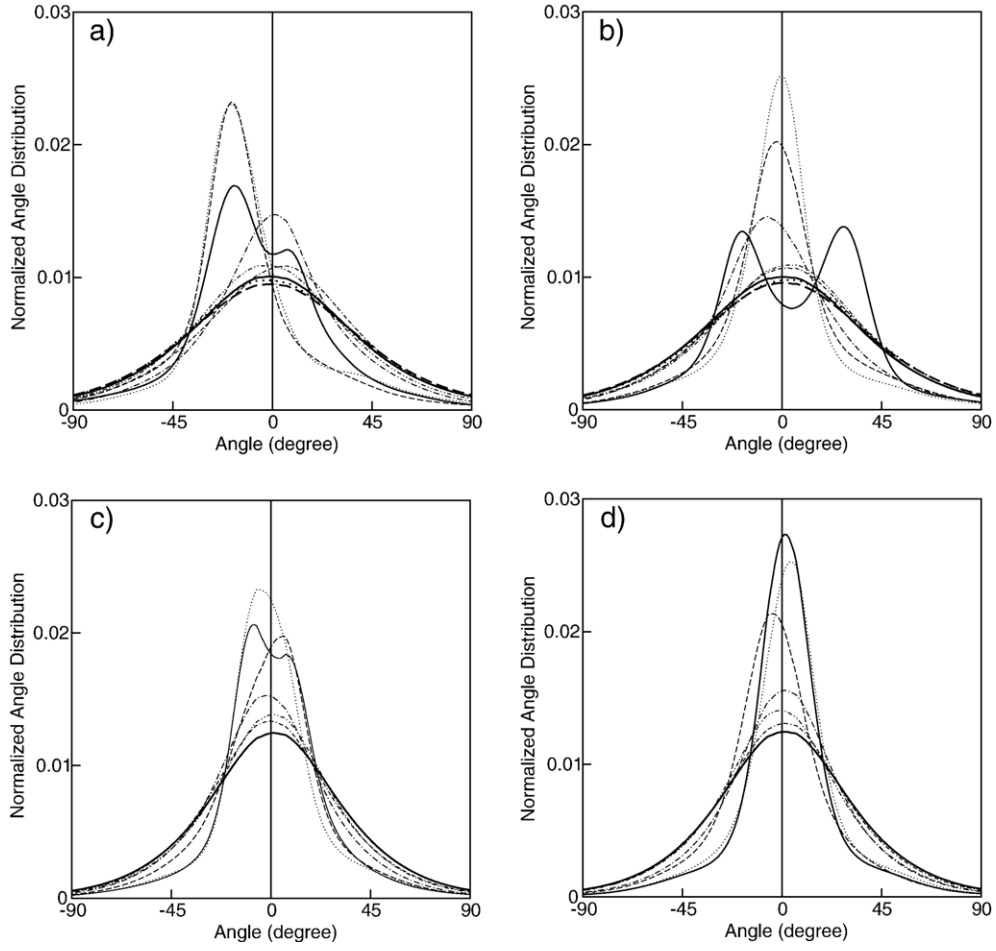

Fig. 7. Normalized angle distribution for all the carbon segments in the lipid tails of DPPC (a and b) and DPPE (c and d). Calculations were performed with respect to the view plane of the simulation box: *xz*-plane (a and c) and *yz*-plane (b and d). Angle is measured with respect to the bilayer normal. For DPPC, the lines correspond to: 250 K (solid), 280 K (dot), 290 K (dash), 300 K (dot-dash), 310 K (dot-dot-dash), 320 K (dot-dash-dash), 330 K (bold-solid), 340 K (bold-dot), and 350 K (bold-dash). For DPPE, the lines correspond to: 290 K (solid), 300 K (dot), 310 K (dash), 320 K (dot-dash), 330 K (dot-dot-dash), 340 K (dot-dash-dash), and 350 K (bold-solid).

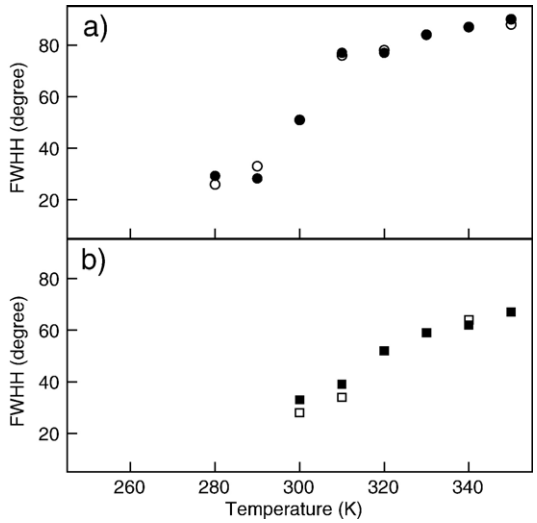

Fig. 8. Calculated full-width at half-height (FWHH) of the distribution curves shown in Fig. 7 for (a) DPPC and (b) DPPE. Close and open symbols correspond to the *xy*- and *yz*-planes, respectively, of the simulation box.

DPPE, since we do not observe a significant jump in the FWHH value at any temperature interval, we conclude that the phase transition for DPPE is related to lesser changes in the lipid configuration in the vicinity of T_m.

The deuterium order parameter, a measure of the orientation and ordering of the lipid tails in the bilayer with respect to the bilayer normal was also calculated to verify the structural changes of the lipid bilayers near the phase transition. The ordering of the tails is expected to change significantly at the phase transition, that is, the alignment of the lipid tails in a gel state is more ordered (higher $|S_{CD}|$ value) than those in a liquid-crystalline state. Fig. 9 shows the average order parameter of the two lipid tails for DPPC and DPPE (see Fig. S3 in the Supplementary Material for a plot with the mean order parameter at each temperature). For DPPC (Fig. 9a), we observe a decrease in the order parameter from 280 to 250 K, which is in part caused by the tilt of lipid tails at 250 K. Between 280 and 300 K, the lipid tails have high values for the order parameter suggesting that these systems are well aligned with the bilayer normal. This is in agreement with the structures shown in Fig. 3 which explains the lowering of the area per lipid. For systems above 310 K, the ordering of the lipid tails decrease with increasing temperature; this is in part due to the increase movement of the lipid tails at high temperature. Note that there is a drastic jump in the order parameter in the temperature range between 300 and 310 K, leading us to conclude that the change is associated with a phase transition for DPPC. Similarly to DPPC, the order parameter for DPPE decreases with increasing temperature; however, the decrease is uniform (see Fig. 9b), which is related to slight changes in the ordering of DPPE due to the tight packing of lipid tails near the transition temperature.

The hydrocarbon *trans-gauche* isomerization has also been used to determine the phase transition of various lipids [49]. In general, the lipid tails in the gel state are predominantly as *trans* conformers, whereas both *trans* and *gauche* conformers are present in a liquid-crystalline state. At low temperatures, the *trans* conformations are preferred because they are energetically more favorable for the lipids in the bilayer arrangement. As the temperature increases to above the phase transition point, the carbon atoms in the lipid tails are less restricted to move, thus creating defects in the hydrocarbon tails (*gauche* formation). As the bilayer transitions from a gel to a liquid-crystalline phase, one expects a significant change in the number of *trans* and *gauche* conformations, reported as % *gauche*. The %*gauche* was analyzed according to the criteria suggested by Tu et al. [50]. The criteria sets a limit between 0 and 360° in the axial rotation of the second bond of a dihedral, starting from a *cis* conformer at 0° to a *trans* conformer at 180°. Based on this criteria, a *gauche* conformation would consist of angles ranging from 0 to 120 and 240 to 360°. Fig. 10 shows the average %*gauche* formed along the lipid tails for DPPC and DPPE at various temperatures (see Fig. S4 in the Supplementary Material for more information on the %*gauche* formed along the lipid tails). As seen in the figure, the %*gauche* increases with increasing temperature. For DPPC, we identified three regions corresponding to the temperature ranges

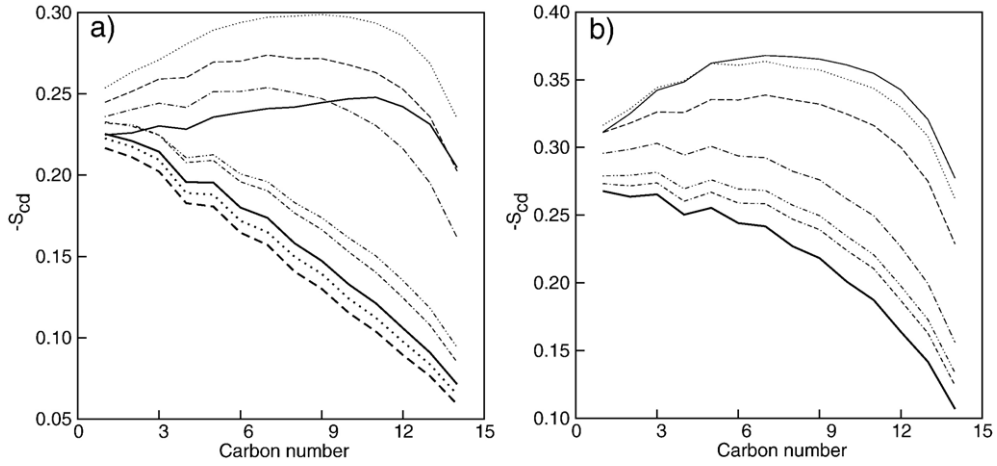

Fig. 9. Lipid tail deuterium order parameter for (a) DPPC and (b) DPPE. Lines representation are described in the caption of Fig. 7.

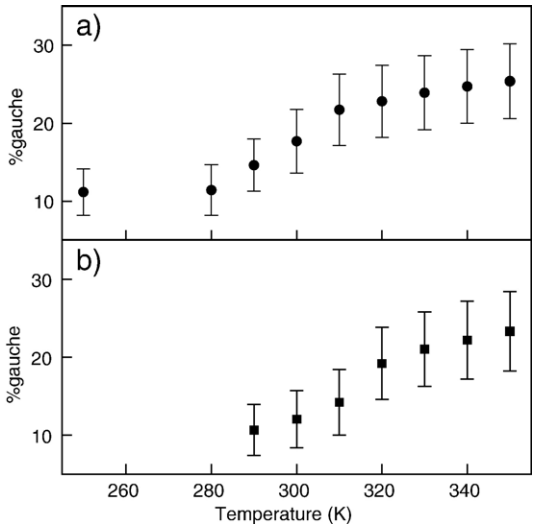

Fig. 10. Average %*gauche* formed along the lipid tails for (a) DPPC and (b) DPPE. Error bars are estimated standard deviation.

of 250–280 K, 280–310 K, and 310–350 K (see Fig. 10a). Since the DPPC bilayers are in a "mixed" phase between 250 and 300 K (see Fig. 3), we can discard the possibility that the discontinuity at 280 K in the %*gauche* distribution corresponds to a phase transition. Therefore, the discontinuity from 300 to 310 K is most likely associated with the main phase transition. Again, this is consistent with the previous analysis. For DPPE, a large discontinuity occurs between 310 and 320 K, which is a reasonable estimate for the phase transition temperature, which is again consistent with the findings discussed previously.

The last quantity we considered to characterize the bilayer systems is the transformation from partial (gel phase) to mixed (liquid-crystalline phase) interdigitation near the phase transition, as described by Chen et al. [22]. Partial interdigitation refers to the chain mismatch of the two leaflets that is, at most, three methylene units from the terminal carbon of the lipid tail (the bilayer thickness is approximately the sum of the acyl chain length of each leaflet [51,52]). This is seen from DPPE at 290 K in Fig. 4, where the terminal carbon of the lipid tails of each leaflet do not overlap one another. Note that the bilayer thickness in this configuration is about the sum of the fully stretched lipid molecules in the two leaflets. On the other hand, mixed interdigitation refers to more overlap, which is commonly seen in lipid bilayers in a liquid-crystalline state. To verify this, we measured the overlap between the lipid tails from opposite leaflets by computing the density profile of the

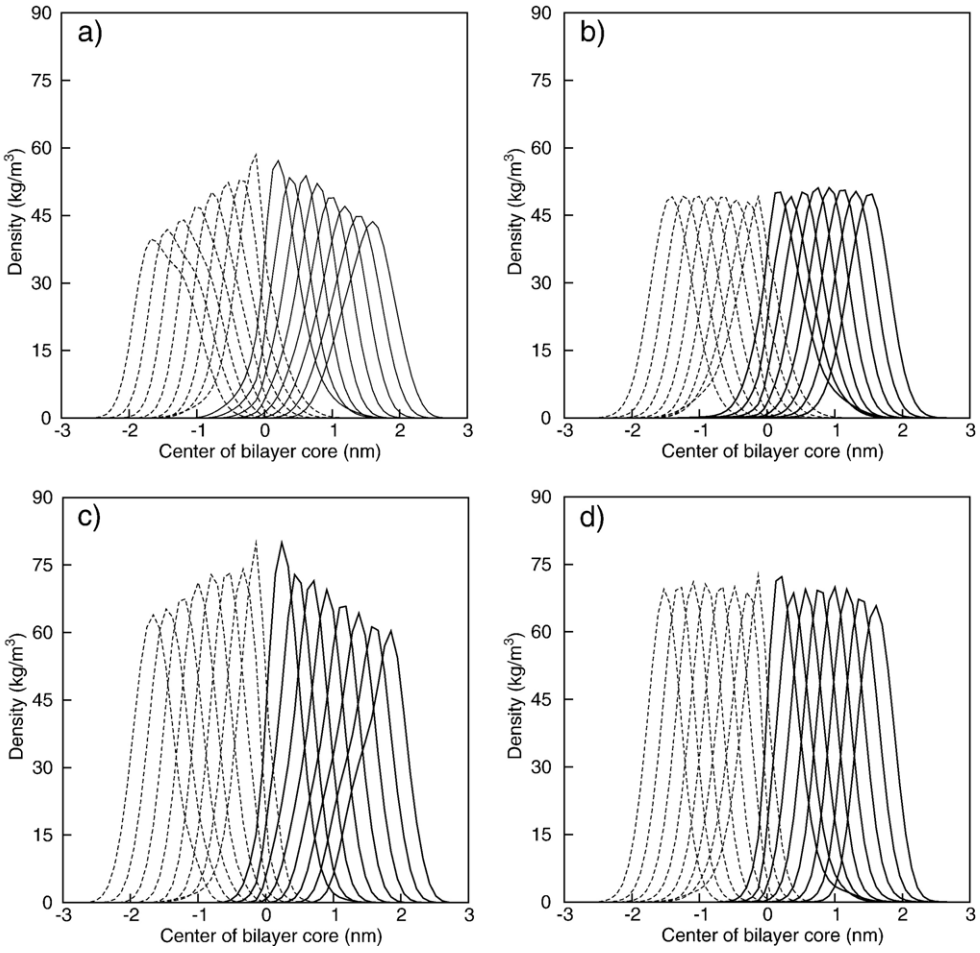

Fig. 11. Density profile for each carbon segment in the *Sn*-2 tail for DPPC at (a) 300 K and (b) 310 K and for DPPE at (c) 310 K and (d) 320 K. Profiles are centered with respect to the middle of the bilayer core. Solid and dash lines represent density profiles for each leaflet.

individual carbon atoms in the acyl chains, as described by Flack et al. [10]. Fig. 11 shows the acyl chain density profiles of DPPC from 300 to 310 K and DPPE from 310 to 320 K. These temperature ranges were chosen because we identified them to cover the phase transition region for DPPC and DPPE. For clarity, we only consider the alternating carbon atoms of the *Sn*-2 tail (the density profile for the *Sn*-1 tails are nearly identical — data not shown here). As seen in the plots, the density profiles are very distinct above and below the phase transition temperature. For DPPC below T_m (Fig. 11a), the density profiles are broad away from the center of bilayer and become narrower near the center. A broad density profile suggests that DPPC has a "mixed" phase with partial and mixed interdigitation co-existing. A narrow density profile of the terminal carbon atoms indicates that lipid tails are not predominantly overlapping. Above T_m (Fig. 11b), the density profiles for all carbon atoms are uniform, suggesting that the lipid tails are fully random and the lipid molecules are evenly distributed in the bilayer. Note that the density profile for the terminal carbon atoms does not show a narrow distribution, unlike the structure below T_m , indicating overlap between the lipid tails of opposite leaflets. Similar results were observed for DPPE above and below T_m . For the density profiles below T_m, the distributions are relatively narrow (Fig. 11c), suggesting an absence of a "mixed" phase. Above T_m, the density profiles show limited overlap of the lipid tails, as indicated by the distribution of the terminal carbon atom (Fig. 11d).

4. Conclusions

Ordered and disordered domains co-exist within biological membrane for many reasons. These domains are structural components that are associated with several biological processes, such as, signal transduction, protein transport, membrane sorting, and membrane binding site. Recently, the study of phase behavior of lipid bilayers has become more apparent with computational methods, especially through the development of coarse-grained models. Coarse-grained models remove some systems size and simulation time limitations that are often associated with atomistic simulations, and as such, they are attractive to study phase separation and domain formation. While coarse-grained models are computationally efficient, they lack in detail to describe important features and characteristics of lipid bilayer at the atomistic scale that contribute to the overall properties of lipid bilayers. This study addresses that missing gap with a comprehensive evaluation of lipid bilayers properties, in particular pertaining to their phase behavior.

MD simulations were performed to investigate the structural properties of DPPC and DPPE bilayers, two of the most abundant lipid components found in living organisms. We considered two sets of lipid bilayer sizes, one containing 256 lipids (128 per leaflet) and another with 128 lipids (64 per leaflet). Even though these bilayers are much smaller than previous study with coarse-grained models, we demonstrate that they are sufficient to yield a wealth of structural information on the bilayers and insight into the mechanism of phase transition from a gel ("ordered") to a liquid-crystalline ("disordered") state. Two sets of simulations were carried out: annealing simulations with continuous heating and cooling, and fixed temperature. The annealing simulations provided a first measure of the structural changes of the bilayers by tracing the hysteresis loop from an ordered to a disordered state. The area per lipid and bilayer thickness were used to obtain an estimate of the first-order phase transition temperature, which was identified at about 305 K and 320 K for DPPC and DPPE bilayers, respectively, compared to the experimental values of 315 K for DPPC and 337 K for DPPE.

In the second set of simulations at fixed temperatures, equilibrium properties were calculated for temperatures above and below the estimated T_m from the annealing simulations. The area per lipid and bilayer thickness measured from the fixed temperature runs were in consistent agreement to those observed in the annealing simulations, with values within the bounds of the hysteresis loop. The resulting equilibrium structure for DPPC below T_m showed "mixed" domains, which consist of lipids that are tilted in the "ordered" domain and partially overlapped in the "disordered" domain. Near T_m, a cooperative transformation of the bilayer structure is observed. First, the average area per lipid slightly increases with increasing temperature, followed by a rearrangement of the lipid tails, resulting in a more "ordered" state and a slightly increase in the membrane thickness. The alignment of lipid tails in this state is predominantly tilted with small tilted-angles, in support to the findings by Ruocco et al., in which a tilted lipid arrangement was reported in the gel phase and a more parallel alignment to the bilayer normal near the transition temperature [48]. Above T_m, the bilayer structure was characterized by the lipid tails able to freely move in random motion, resulting in an increase in the %*gauche* formed and an increase in the level of interdigitation between lipids in opposite leaflets.

The phase transformation for DPPE was similar to that of DPPC, except that, because of its structural property (smaller headgroup), bilayer below T_m consisted primarily of "ordered" domains. The smaller area per lipid of DPPE is reflected in the tight packing of the lipids, and in turn, with small tilted-angles. In agreement with the hysteresis loop from the annealing simulations, the DPPE bilayer structure experienced minimal rearrangement of the lipids, as the bilayer thickness gradually decrease near the phase transition. These results support the study by Yao et al. in which they were unable to distinguish a stable phase from a gel to a liquid-crystalline phase for DPPE [46]. Near T_m , cooperative structural changes were observed with a decrease in the ordering of the lipid tails and an increase in the %*gauche* formation and level of interdigitation. Because the DPPE molecules remain closely packed at above T_m , the lipid tails do not overlap, which is confirmed by the density profile of the terminal carbon atoms.

In summary, the mechanism for phase transition from a gel to a liquid-crystalline phase for DPPC and DPPE bilayers involves cooperative changes of bilayer structure that can be quantified with the area per lipid, bilayer thickness, lipid tail tilt-angle, lipid tail order parameter, hydrocarbon *trans-gauche* isomerization, and level of interdigitation. The implication of all the structural changes observed supports a first-order phase

transition for DPPC and DPPE that are in reasonable agreement with experimental values.

This study demonstrates that one can use atomistic simulations to obtain important information of lipid bilayers at and near the main transition state (gel to liquid-crystalline). This study also provides insight into the structural changes that DPPC and DPPE bilayers undergo in the phase transition from a gel to a liquid-crystalline state. Moreover, the properties analyzed give valuable structural data to understand the mechanism underlying phase transitions, which may not be readily accessible from experimental measurements.

Supplementary material

Supplementary data associated with this article can be found, in the online version, at doi:10.1016/j.bbamem.2006.11.003.

Acknowledgements

Computational resources were provided by the Virginia Tech Terascale Computing Facility (System X). We are very grateful to the reviewers for their insightful comments.

References

[1] E. London, How principles of domain formation in model membranes may explain ambiguities concerning lipid raft formation in cells, Biochim. Biophys. Acta, Mol. Cell Res. 1746 (3) (2005) 203–220.
[2] D.A. Brown, E. London, Functions of lipid rafts in biological membranes, Annu. Rev. Cell Dev. Biol. 14 (1998) 111–136.
[3] K. Simons, D. Toomre, Lipid rafts and signal transduction, Nat. Rev., Mol. Cell Biol. 2 (3) (2001) 216.
[4] K. Simons, E. Ikonen, Functional rafts in cell membranes, Nature 387 (6633) (1997) 569–572.
[5] E. Ikonen, Roles of lipid rafts in membrane transport, Curr. Opin. Cell Biol. 13 (4) (2001) 470–477.
[6] J. Herreros, T. Ng, G. Schiavo, Lipid rafts act as specialized domains for tetanus toxin binding and internalization into neurons, Mol. Biol. Cell 12 (10) (2001) 2947–2960.
[7] J. Fantini, N. Garmy, R. Mahfoud, N. Yahi, Lipid rafts: structure, function and role in HIV, Alzheimers and prion diseases, Expert Rev. Mol. Med. 2002 (2002) 1–22.
[8] F. Lafont, G. van der Goot, Bacterial invasion via lipid rafts, Cell Microbiol. 7 (5) (2005) 613–620.
[9] C. Hofsäβ, E. Lindahl, O. Edholm, Molecular dynamics simulations of phospholipid bilayers with cholesterol, Biophys. J. 84 (4) (2003) 2192–2206.
[10] E. Falck, M. Patra, M. Karttunen, T. Hyvonen, I. Vattulainen, Lessons of slicing membranes: interplay of packing, free area, and lateral diffusion in phospholipid/cholesterol bilayers, Biophys. J. 87 (2) (2004) 1076–1091.
[11] S.A. Pandit, E. Jakobsson, H.L. Scott, Simulation of the early stages of nano-domain formation in mixed bilayers of sphingomyelin, cholesterol, and dioleylphosphatidylcholine, Biophys. J. 87 (5) (2004) 3312–3322.
[12] J. Suurkuusk, B.R. Lentz, Y. Barenholz, R.L. Biltonen, T.E. Thompson, A calorimetric and fluorescent probe study of the gel–liquid crystalline phase transition in small, single-lamellar dipalmitoylphosphatidylcholine vesicles, Biochemistry 15 (7) (1976) 1393–1401.
[13] J.H. Davis, Deuterium magnetic resonance study of the gel and liquid crystalline phases of dipalmitoyl phosphatidylcholine, Biophys. J. 27 (3) (1979) 339–358.
[14] C. Huang, S. Li, Calorimetric and molecular mechanics studies of the thermotropic phase behavior of membrane phospholipids, Biochim. Biophys. Acta, Biomembr. 1422 (3) (1999) 273–307.
[15] J.F. Nagle, S. Tristram-Nagle, Structure of lipid bilayers, Biochim. Biophys. Acta, Rev. Biomembr. 1469 (3) (2000) 159–195.
[16] A.J. Metso, A. Jutila, J.P. Mattila, J.M. Holopainen, P.K.J. Kinnunen, Nature of the main transition of diphanitoylphosphocholine bilayers inferred from fluorescence spectroscopy, J. Phys. Chem. B 107 (5) (2003) 1251–1257.
[17] M. Kusube, M. Goto, N. Tamai, H. Matsuki, S. Kaneshina, Bilayer phase transitions of N-methylated dioleoylphosphatidylethanolamines under high pressure, Chem. Phys. Lipids 142 (1–2) (2006) 94–102.
[18] O.G. Mouritsen, A. Boothroyd, R. Harris, N. Jan, T. Lookman, L. MacDonald, D.A. Pink, M.J. Zuckermann, Computer simulation of the main gel–fluid phase transition of lipid bilayers, J. Chem. Phys. 79 (4) (1983) 2027–2041.
[19] M. Nielsen, L. Miao, J.H. Ipsen, M.J. Zuckermann, O.G. Mouritsen, Off-lattice model for the phase behavior of lipid–cholesterol bilayers, Phys. Rev. E 59 (5) (1999) 5790–5803.
[20] J.M. Polson, I. Vattulainen, H. Zhu, H. Zuckermann, Simulation study of lateral diffusion in lipid–sterol bilayer mixtures, Eur. Phys. J., E 5 (4) (2001) 485–497.
[21] G. Brannigan, A.C. Tamboli, F.L. Brown, The role of molecular shape in bilayer elasticity and phase behavior, J. Chem. Phys. 121 (7) (2004) 3259–3271.
[22] L.B. Chen, M.L. Johnson, R.L. Biltonen, A macroscopic description of lipid bilayer phase transitions of mixed-chain phosphatidylcholines: chain-length and chain-asymmetry dependence, Biophys. J. 80 (1) (2001) 254–270.
[23] M. Kranenburg, M. Venturoli, B. Smit, Phase behavior and induced interdigitation in bilayers studied with dissipative particle dynamics, J. Phys. Chem. B 107 (41) (2003) 11491–11501.
[24] H. Heller, M. Schaefer, K. Schulten, Molecular-dynamics simulation of a bilayer of 200 lipids in the gel and in the liquid-crystal phases, J. Phys. Chem. 97 (31) (1993) 8343–8360.
[25] R.M. Venable, B.R. Brooks, R.W. Pastor, Molecular dynamics simulations of gel ($L_{\beta I}$) phase lipid bilayers in constant pressure and constant surface area ensembles, J. Chem. Phys. 112 (10) (2000) 4822–4832.
[26] A.H. de Vries, S. Yefimov, A.E. Mark, S.J. Marrink, Molecular structure of the lecithin ripple phase, Proc. Natl. Acad. Sci. U. S. A. 102 (15) (2005) 5392–5396.
[27] M.J. Stevens, Coarse-grained simulations of lipid bilayers, J. Chem. Phys. 121 (23) (2004) 11942–11948.
[28] S.J. Marrink, J. Risselada, A.E. Mark, Simulation of gel phase formation and melting in lipid bilayers using a coarse grained model, Chem. Phys. Lipids 135 (2) (2005) 223–244.
[29] M.J. Janiak, D.M. Small, G.G. Shipley, Nature of the thermal pretransition of synthetic phospholipids: dimyristolyl- and dipalmitoyllecithin, Biochemistry 15 (21) (1976) 4575–4580.
[30] A.G. Petrov, K. Gawrisch, G. Brezesinski, G. Klose, A. Möps, Optical detection of phase transitions in simple and mixed lipid–water phases, Biochim. Biophys. Acta, Biomembr. 690 (1) (1982) 1–7.
[31] S. Leekumjorn, A.K. Sum, Molecular simulation study of structural and dynamic properties of mixed DPPC/DPPE bilayers, Biophys. J. 90 (11) (2006) 3951–3965.
[32] E. Egberts, S.J. Marrink, H.J.C. Berendsen, Molecular dynamics simulation of a phospholipid membrane, Eur. Biophys. J. 22 (6) (1994) 423–436.
[33] W.F. van Gunsteren, S.R. Billeter, A.A. Eising, P.H. Hünenberger, P. Krüger, A.E. Mark, W.R.P. Scott, I.G. Tironi, Biomolecular simulation: the GROMOS96 manual and user guide, vdf Hochschuleverlag AG an der ETH Zürich, Zürich, Switzerland, 1996.
[34] J.P. Ryckaert, A. Bellemans, Molecular dynamics of liquid *n*-butane near its boiling point, Chem. Phys. Lett. 30 (1) (1975) 123–125.
[35] O. Berger, O. Edholm, F. Jähnig, Molecular dynamics simulations of a fluid bilayer of dipalmitoylphosphatidylcholine at full hydration, constant pressure, and constant temperature, Biophys. J. 72 (5) (1997) 2002–2013.
[36] W.L. Jorgensen, J. Tirado-Rives, The OPLS potential function for proteins. Energy minimizations for crystals of cyclic peptides and crambin, J. Am. Chem. Soc. 110 (1988) 1657–1666.
[37] J.W. Essex, M.M. Hann, W.G. Richards, Molecular dynamics simulation of a hydrated phospholipid bilayer, Philos. Trans. R. Soc., B 344 (1309) (1994) 239–260.

[38] S.W. Chiu, M. Clark, V. Balaji, S. Subramaniam, H.L. Scott, E. Jakobsson, Incorporation of surface tension into molecular dynamics simulation of an interface: a fluid phase lipid bilayer membrane, Biophys. J. 69 (4) (1995) 1230–1245.
[39] H.J.C. Berendsen, J.P.M. Postma, W.F. van Gunsteren, J. Hermans, Intermolecular Forces, Reidel, Dordrecht, The Netherlands, 1981.
[40] T. Darden, D. York, L. Pedersen, Particle mesh Ewald: an $N\log(N)$ method for Ewald sums in large systems, J. Chem. Phys. 98 (1993) 10089–10092.
[41] U. Essman, L. Perera, M.L. Berkowitz, T. Darden, H. Lee, L.G. Pedersen, A smooth particle mesh Ewald method, J. Chem. Phys. 103 (1995) 8577–8593.
[42] H.J.C. Berendsen, D. van der Spoel, R. van Drunen, GROMACS: a message-passing parallel molecular dynamics implementation, Comput. Phys. Commun. 91 (1–3) (1995) 43–56.
[43] E. Lindahl, B. Hess, D. van der Spoel, GROMACS 3.0: a package for molecular simulation and trajectory analysis, J. Mol. Model. 7 (8) (2001) 306–317.
[44] Virginia Tech, http://www.tcf.vt.edu (Terascale Computing Facility).
[45] T. Chen, J.P. Acker, A. Eroglu, S. Cheley, H. Bayley, A. Fowler, M.L. Toner, Beneficial effect of intracellular trehalose on the membrane integrity of dried mammalian cells, Cryobiology 43 (2) (2001) 168–181.
[46] H. Yao, I. Hatta, R. Koynova, B. Tenchov, Time-resolved X-ray diffraction and calorimetric studies at low scan rates. On the fine structure of the phase transitions in hydrated dipalmitoylphosphatidylethanolamine, Biophys. J. 61 (3) (1992) 683–693.
[47] A.K. Sum, R. Faller, J.J. de Pablo, Molecular simulation study of phospholipid bilayers and insights of the interactions with disaccharides, Biophys. J. 85 (5) (2003) 2830–2844.
[48] M.J. Ruocco, G.G. Shipley, Characterization of the sub-transition of hydrated dipalmitoylphosphatidylcholine bilayers. X-ray diffraction study, Biochim. Biophys. Acta, Biomembr. 684 (1) (1982) 59–66.
[49] N. Yellin, I.W. Levin, Hydrocarbon chain *trans-gauche* isomerization in phospholipid bilayer gel assemblies, Biochemistry 16 (4) (1977) 642–647.
[50] K. Tu, D.J. Tobias, J.K. Blasie, M.L. Klein, Molecular dynamics investigation of the structure of a fully hydrated gel-phase dipalmitoylphosphatidylcholine bilayer, Biophys. J. 70 (2) (1996) 595–608.
[51] J.T. Mason, C. Huang, R.L. Biltonen, Calorimetric investigations of saturated mixed-chain phosphatidylcholine bilayer dispersions, Biochemistry 20 (21) (1981) 6086–6092.
[52] C. Huang, J.T. Mason, I.W. Levin, Raman spectroscopic study of saturated mixed-chain phosphatidylcholine multilamellar dispersions, Biochemistry 22 (11) (1983) 2775–2780.